International Journal of Engineering Technology, Management and Applied Sciences

www.ijetmas.com June 2015, Volume 3, Issue 6, ISSN 2349-4476

Speed Control of Brushless DC Motor Using Microcontroller

R Giridhar Balakrishna
Assistant Professor
VR Siddhartha Engineering college,
Vijayawada, A.P.,India

P Yogananda Reddy
Assistant Professor
VR Siddhartha Engineering college,
Vijayawada, A.P.,India

ABSTRACT

In this paper we are designing a low cost microcontroller based speed control of BLDC motor. A DC Brushless Motor uses a permanent magnet external rotor, three phase of driving coils, one or more Hall Effect devices are used to sense the position of rotor, and the associated drive electronics. The coils are activated, one phase after the other, by the drive electronics as queued by the signals from the Hall effect sensors, they act as three phase synchronous motors containing their own variable frequency drive electronics.

1. INTRODUCTION

The economic constraints and new standards legislated by governments place increasingly stringent requirements on electrical systems. New generations of equipment must have higher performance parameters such as better efficiency and reduced electromagnetic interference. System flexibility must be high to facilitate market modifications and to reduce development time. All these improvements must be achieved while, at the same time, decreasing system cost. Brushless motor technology makes it possible to achieve these specifications. Such motors combine high reliability with high efficiency, and for a lower cost in comparison with brush motors. This paper describes the use of a Brushless DC Motor (BLDC). Although the brushless characteristic can be apply to several kinds of motors – AC synchronous motors, stepper motors, switched reluctance motors, AC induction motors - the BLDC motor is conventionally defined as a permanent magnet synchronous motor with a trapezoidal Back EMF waveform shape. Permanent magnet synchronous machines with trapezoidal Back-EMF and (120 electrical degrees wide) rectangular stator currents are widely used as they offer the following advantages first, assuming the motor has pure trapezoidal Back EMF and that the stator phases commutation process is accurate, the mechanical torque developed by the motor is constant; secondly, the Brushless DC drives show a very high mechanical power density.

1.1 BLDC MOTOR BACKGROUND

BLDC motor drives, systems in which a permanent magnet excited synchronous motor is fed with a variable frequency inverter controlled by a shaft position sensor. There appears a lack of commercial simulation packages for the design of controller for such BLDC motor drives. One main reason has been that the high software development cost incurred is not justified for their typical low cost fractional/integral kW application areas such as NC machine tools and robot drives, even it could imply the possibility of demagnetizing the rotor magnets during commissioning or tuning stages. Nevertheless, recursive prototyping of both the motor and inverter may be involved in novel drive configurations for advance and specialized applications, resulting in high developmental cost of the drive system. Improved magnet material with high (B.H), product also helps push the BLDC motors market to tens of kW application areas where commissioning errors

www.ijetmas.com June 2015, Volume 3, Issue 6, ISSN 2349-4476

become prohibitively costly. Modeling is therefore essential and may offer potential cost savings.

A brushless dc motor is a dc motor turned inside out, so that the field is on the rotor and the armature is on the stator. The brushless dc motor is actually a permanent magnet ac motor whose torque "current characteristics mimic the dc motor. Instead of commutating the armature current using brushes, electronic commutation is used. This eliminates the problems associated with the brush and the commutator arrangement, for example, sparking and wearing out of the commutator" brush arrangement, thereby, making a BLDC more rugged as compared to a dc motor. Having the armature on the stator makes it easy to conduct heat away from the windings, and if desired, having cooling arrangement for the armature windings is much easier as compared to a dc motor.

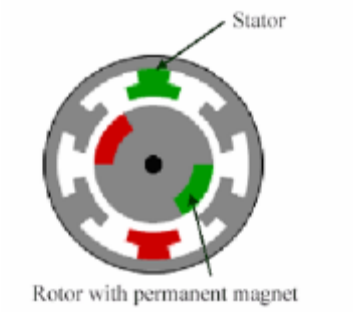

Fig 1.1 Cross-section view of a brushless dc motor

In effect, a BLDC motor is a modified PMSM motor with the modification being that the back Emf is trapezoidal instead of being sinusoidal as in the case of PMSM. The “Commutation region” of the back Emf of a BLDC motor should be as small as possible, while at the same time it should not be so narrow as to make it difficult to commutate a phase of that motor when driven bya Current Source Inverter. The flat constant portion of the back Emf should be 120° for a smooth torque production.

2. BLDC MOTOR DYNAMIC MODEL AND GENERALITIES

2.1 Introduction

The steady-state model and equivalent circuit are useful for studying the performance of machine in steady state. This implies that all electrical transients are neglected during load changes and stator frequency variations. Such variations arise in applications involving variable-speed drives. The dynamic model considers the instantaneous effects of varying voltages/currents, stator frequency and torque disturbances.

2.2 Dynamic Model of Induction Machine

The BLDC Motor has three stator windings and a permanent magnet rotor on the rotor. Rotor induced currents can be neglected due to the high resistivity of both magnets and stainless steel. No damper winding are modeled the circuit equation of the three windings in phase variables are obtained.

$$\begin{pmatrix} Vas \\ Vbs \\ Vcs \end{pmatrix} = \begin{pmatrix} Rs & 0 & 0 \\ 0 & Rs & 0 \\ 0 & 0 & Rs \end{pmatrix} \begin{pmatrix} Ia \\ Ib \\ Ic \end{pmatrix} + \frac{dx}{dt} \begin{bmatrix} Laa & Lab & Lac \\ Lba & Lbb & Lbc \\ Lca & Lcb & Lcc \end{bmatrix} \quad (2.1)$$

whereas Vas, Vbs and Vcs are the stator phase voltages; R is the stator resistance per phase;Ia,Ib and Icare the stator phase currents Laa,Lbb and Lcc are the self-inductance of phases a, b and c;Lab, Lbcand Lac are the mutual inductances between phases a, b and c; Ea,Eb and Ec are the phase back electromotive forces .It has been assumed that resistance of all the winding are equal. It also has been assumed that if there is no change in the rotor reluctance with angle because of a no salient rotor and then

$$Laa = Lbb = Lcc = L \quad (2.2)$$

$$Lab = Lba = Lac = Lca = Lbc = Lcb = M \quad (2.3)$$

Substituting the equations (2.2) and (2.3) in equation (2.1) gives the PMBLDCM model as

$$\begin{pmatrix} Vas \\ Vbs \\ Vcs \end{pmatrix} = \begin{pmatrix} Rs & 0 & 0 \\ 0 & Rs & 0 \\ 0 & 0 & Rs \end{pmatrix} \begin{pmatrix} Ia \\ Ib \\ Ic \end{pmatrix} + \frac{dx}{dt} \begin{bmatrix} L & M & M \\ M & L & M \\ M & M & L \end{bmatrix} \begin{pmatrix} Ia \\ Ib \\ Ic \end{pmatrix} + \begin{pmatrix} Ea \\ Eb \\ Ec \end{pmatrix} \quad (2.4)$$

www.ijetmas.com June 2015, Volume 3, Issue 6, ISSN 2349-4476

Whereas Vas, Vbs and Vcs are phase voltages and may be designed as

$$Vas = Vaa - Vno, Vbs = Vba - Vno, Vcs = Vca - Vno \quad (2.5)$$

Where Vao, Vbo, Vco and Vno are three phase and neutral voltages referred to the zero reference potential at the midpoint of dc link.

The stator phase currents are constrained to be balanced i.e.

$$Ia + Ib + Ic = 0 \quad (2.6)$$

This leads to the simplifications of the inductances matrix in the models as then

$$MIa + MIb + MIc = 0 \quad (2.7)$$

Therefore in state space from

$$\begin{pmatrix} Vas \\ Vbs \\ Vcs \end{pmatrix} = \begin{pmatrix} Rs & 0 & 0 \\ 0 & Rs & 0 \\ 0 & 0 & Rs \end{pmatrix} \begin{pmatrix} Ia \\ Ib \\ Ic \end{pmatrix} + \frac{dx}{dt} \begin{bmatrix} L-M & 0 & 0 \\ 0 & L-M & 0 \\ 0 & 0 & L-M \end{bmatrix} \begin{pmatrix} Ia \\ Ib \\ Ic \end{pmatrix} + \begin{pmatrix} Ea \\ Eb \\ Ec \end{pmatrix}$$

It has been assumed that back EMF Ea, Eb and Ec are having trapezoidal waveform

$$\begin{pmatrix} Ea \\ Eb \\ Ec \end{pmatrix} = \omega m \lambda m \begin{pmatrix} fas(\theta r) \\ fbs(\theta r) \\ fcs(\theta r) \end{pmatrix} \quad (2.8)$$

Where ωm the angular rotor speed in radians per seconds, λm is the flux linkage, θr is the rotor position in radian and the functions fas(θr), fbs(θr) and fcs(θr) have the same shape as Ea, Eb and Ec with a maximum magnitude of ± 1. The induced emf's do not have sharp corners because these are in trapezoidal nature.

The emf's are the result of the flux linkages derivatives and the flux linkages are continuous function. Fringing also makes the flux density function smooth with no abrupt edges.

The electromagnetic toque in Newton's defined as

$$Te = [EaIa + EbIb + EcIc]/\omega m \quad (2.9)$$

It is significant to observe that the phase voltage equation is identical to armature voltage equation of dc machine. That is one of reasons for naming this machine the PM brushless dc machine.

The moment of inertia is described as

$$J = Jm + Jl \quad (2.10)$$

The equation of the simple motion system with inertia J, friction coefficient B, and load Torque Tl is

$$J\frac{d\omega}{dt} + B\omega m = (Te - Tl) \quad (2.11)$$

The electrical rotor speed and position are related by

$$\frac{d\theta r}{dt} = \frac{p}{2}\omega m \quad (2.12)$$

The damping coefficient B is generally small and often neglected thus the system. The above equation is the rotor position θr and it repeats every 2π. The potential of the neutral point with respect to the zero potential (Vno) is required to be considered in order to avoid imbalance in the applied voltage and simulate the performance of the drive. This is obtained by substituting equation (2.6) in the volt ampere equation (2.8) and adding then give as

$$Vao + Vbo + Vco - 3Vn0 = Rs(Ia + Ib + Ic) + (L - M)(pIa + pIb + pIc) + (Ea + Eb + Ec) \quad (2.13)$$

Substituting equation (2.6) in equation (2.14) we get

$$Vao + Vbo + Vco - 3Vn0 = (Ea + Eb + Ec) \quad (2.14)$$

Thus

$$Vno = [[Vao + Vbo + Vco] - (Ea + Eb + Ec)]/3 \quad (2.15)$$

The set of differential equations mentioned in equations (2.8), (2.12), and (2.13), defines the developed model in terms of the variables Ia, Ib, Ic, ωm and, θr time as an independent variable.

Combining the all relevant equations, the system in state space form is

$$\dot{x} = Ax + Bx + Ce \quad (2.16)$$

Where

$$x = [Ia\ Ib\ Ic\ \omega m\ \theta r] \quad (2.17)$$

$$A = \begin{bmatrix} -\frac{R_s}{L-M} & 0 & 0 & -\frac{\lambda_m}{J} f_a(\theta_r) & 0 \\ 0 & -\frac{R_s}{L-M} & 0 & -\frac{\lambda_m}{J} f_b(\theta_r) & 0 \\ 0 & 0 & -\frac{R_s}{L-M} & -\frac{\lambda_m}{J} f_c(\theta_r) & 0 \\ \frac{\lambda_m}{J} f_a(\theta_r) & \frac{\lambda_m}{J} f_b(\theta_r) & \frac{\lambda_m}{J} f_c(\theta_r) & -\frac{B}{J} & 0 \\ 0 & 0 & 0 & \frac{P}{2} & 0 \end{bmatrix} \quad (2.18)$$

www.ijetmas.com June 2015, Volume 3, Issue 6, ISSN 2349-4476

$$B = \begin{bmatrix} \frac{1}{L-M} & 0 & 0 & 0 \\ 0 & \frac{1}{L-M} & 0 & 0 \\ 0 & 0 & \frac{1}{L-M} & 0 \\ 0 & 0 & 0 & \frac{1}{L-M} \end{bmatrix}$$

$$C = \begin{pmatrix} \frac{-1}{L-M} & 0 & 0 \\ 0 & \frac{-1}{L-M} & 0 \\ 0 & 0 & \frac{-1}{L-M} \end{pmatrix} \quad (2.20)$$

$$U = [Vas \quad Vbs \quad Vcs \quad Tl]^t \quad (2.21)$$

$$E = [Ea \quad Eb \quad Ec]^t \quad (2.22)$$

3.HARDWARE COMPONENTS

The main components required in implementing the project are:

1. Brushless DC Motor
2.Hall Sensors
3.Inverter
4.Microcontroller

3.1 BLDC MOTOR

The BLDC motor is an AC synchronous motor with permanent magnets on the rotor (moving part) and windings on the stator (fix part). Permanent magnets create the rotor flux and the energized stator windings create electromagnet poles. The rotor (equivalent to a bar magnet) is attracted by the energized stator phase. By using the appropriate sequence to supply the stator phases, a rotating field on the stator is created and maintained. This action of the rotor - chasing after the electromagnet poles on the stator - is the fundamental action used in synchronous permanent magnet motors. The lead between the rotor and the rotating field must be controlled to produce torque and this synchronization implies knowledge of the rotor position.

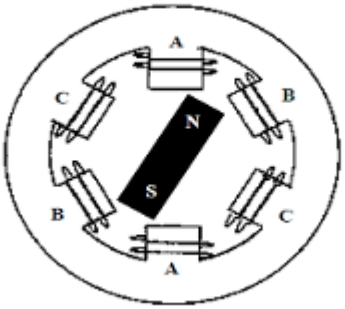

Fig3.1.1 A three-phase synchronous motor with a one permanent magnet pair pole rotor

On the stator side, three phase motors are the most common. These offer a good compromise between precise control and the number of power electronic devices required to control the stator currents. For the rotor, a greater number of poles usually create a greater torque for the same level of current. On the other hand, by adding more magnets, a point is reached where, because of the space needed between magnets, the torque no longer increases. The manufacturing cost also increases with the number of poles. As a consequence, the number of poles is a compromise between cost, torque and volume.

Permanent magnet synchronous motors can be classified in many ways, one of these that is of particular interest to us is that depending on back-emf profiles: Brushless Direct Current Motor (BLDC) and Permanent Magnet Synchronous Motor (PMSM). This terminology defines the shape of the back-emf of the synchronous motor. Both BLDC and PMSM motors have permanent magnets on the rotor but differ in the flux distributions and back-emf profiles.

BLDC MOTOR CONROL

The BLDC motor is characterized by a two phase ON operation to control the inverter. In this control scheme, torque production follows the principle that current should flow in only two of the three phases at a time and that there

www.ijetmas.com June 2015, Volume 3, Issue 6, ISSN 2349-4476

should be no torque production in the region of Back
EMF zero crossings. The following figure describes the electrical wave forms in the BLDC motor in the two phases ON operation.
This control structure has several advantages:
1. Only one current sensor is necessary
2. The positioning of the current sensor allows the use of low cost sensors as a shunt.

We have seen that the principle of the BLDC motor is, at all times, to energize the phase pair which can produce the highest torque. To optimize this effect the Back EMF shape is trapezoidal. The combination of a DC current with a trapezoidal Back EMF makes it theoretically possible to produce a constant torque. In practice, the current cannot be established instantaneously in a motor phase; as a consequence the torque ripple is present at each 60 degree phase commutation.

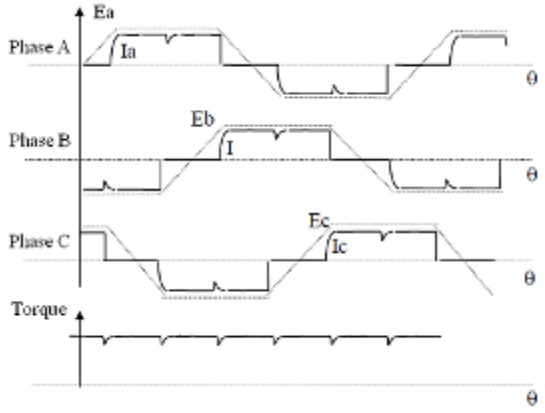

Fig 3.1.2 Electrical Waveforms in the Two Phase ON Operation and Torque Ripple

If the motor used has a sinusoidal Back EMF shape, this control can be applied but the produced torque is:

- Firstly, not constant but made up from portions of a sine wave. This is due to its being thecombination of a trapezoidal current control strategy and of a sinusoidal Back EMF. Bear in mind that a sinusoidal Back EMF shape motor controlled with a sine wave strategy (three phase ON) produces a constant torque.
- Secondly, the torque value produced is weaker.

Fig 3.1.3 Torque Ripple in a Sinusoidal Motor Controlled as a BLDC

3.2 HALL SENSORS

A Hall Effect sensor is a transducer that varies its output voltage in response to a magnetic field. Hall Effect sensors are used for proximity switching, positioning, speed detection, and current sensing applications.
In its simplest form, the sensor operates as an analogue transducer, directly returning a voltage. With a known magnetic field, its distance from the Hall plate can be determined. Using groups of sensors, the relative position of the magnet can be deduced.

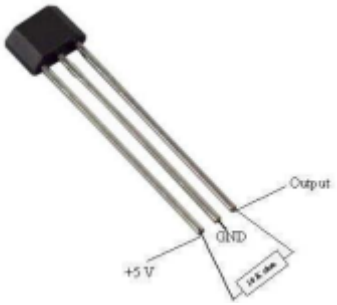

Fig 3.2.1 Hall Sensor

Electricity carried through a conductor will produce a magnetic field that varies with current, and a Hall sensor can be used to measure the current without interrupting the circuit. Typically, the sensor is integrated with a wound core or permanent magnet that surrounds the conductor to be measured.

Frequently, a Hall sensor is combined with circuitry that allows the device to act in a digital (on/off) mode, and may be called a switch in this configuration. Commonly seen in

www.ijetmas.com June 2015, Volume 3, Issue 6, ISSN 2349-4476

industrial applications such as the pictured pneumatic cylinder, they are also used in consumer equipment; for example some computer printers use them to detect missing paper and open covers. When high reliability is required, they are used in keyboards.

Hall sensors are commonly used to time the speed of wheels and shafts, such as for internal combustion engine ignition timing, tachometers and anti-lock braking systems. They are used in brushless DC electric motors to detect the position of the permanent magnet. In the pictured wheel with two equally spaced magnets, the voltage from the sensor will peak twice for each revolution. This arrangement is commonly used to regulate the speed of disc drives.

3.2.1 HALL EFFECT

The Hall Effect is the production of a voltage difference (the Hall voltage) across an electrical conductor, transverse to an electric current in the conductor and a magnetic field perpendicular to the current. It was discovered by Edwin Hall in 1879.

The Hall coefficient is defined as the ratio of the induced electric field to the product of the current density and the applied magnetic field. It is a characteristic of the material from which the conductor is made, since its value depends on the type, number, and properties of the charge carriers that constitute the current.

3.2.2 BASIC BLOCK DIAGRAM AND WORKING

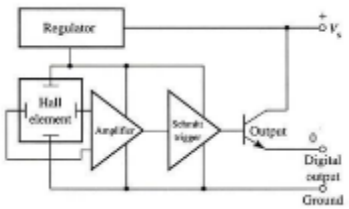

Fig 3.2.2 Blok diagram of Hall sensor

From the figure 3.2.2 we notice that this sensor is a three-wire sensor. This means that two wires, the + V, and the ground provide dc voltage for the power supply portion of the sensor.

Terminal 0 and ground are used as the output terminals for the sensor. Since this is a three-wire sensor, the ground terminal is part of the power supply and part of the output circuit. The power supply uses a voltage regulator to provide the initial current for the Hall-effect element and voltage for the op amp. The small sensor terminals are connected to the op amp input terminals.

When a magnetic field is sensed, a small voltage is sent to the op amp and the output of the Op amp is sent to a Schmitt trigger and then to the base of an NPN transistor. When the base of the transistor is biased, it will go into saturation and current will flow through its emitter-collector circuit to provide a digital (on/off) output signal. In the current-sinking circuit, notice that the transistor provides a path to ground when the transistor is biased to saturation.

3.2.3 HALL PROBE

The Hall probe is a magnetic field sensor that passes electrical current when the sensor is perpendicular to a magnetic field. The stronger the B-Field, the more current it passes. A Hall probe contains an indium compound semiconductor crystal such as indium antimonite, mounted on an aluminum backing plate, and encapsulated in the probe head. The plane of the crystal is perpendicular to the probe handle. Connecting leads from the crystal are brought down through the handle to the circuit box.

When the Hall Probe is held so that the magnetic field lines are passing at right angles through the sensor of the probe, the meter gives a reading of the value of magnetic flux density (B). A current is passed through the crystal which, when placed in a magnetic field has a ―Hall effect‖ voltage developed across it. The Hall Effect is seen when a conductor is passed

www.ijetmas.com June 2015, Volume 3, Issue 6, ISSN 2349-4476

through a uniform magnetic field. The natural electron drift of the charge carriers causes the magnetic field to apply a Lorentz force (the force exerted on a charged particle in an electromagnetic field) to these charge carriers. The result is what is seen as a charge separation, with a buildup of either positive or negative charges on the bottom or on the top of the plate. The crystal measures 5 mm square. The probe handle, being made of a non-ferrous material, has no disturbing effect on the field.

A Hall Probe is enough to measure the Earth's magnetic field. It must be held so that the Earth's field lines are passing directly through it. It is then rotated quickly so the field lines pass through the sensor in the opposite direction. The change in the flux density reading is double the Earth's magnetic flux density. A hall probe must first be calibrated against a known value of magnetic field strength. For a solenoid the hall probe is placed in the center.

3.3 INVERTER

3.3.1 INTRODUCTION

The main objective of an inverter is to produce an ac output waveform from a dc power supply. These are the types of waveforms required in adjustable speed drives (ASDs), uninterruptible power supplies (UPS), static VAR compensators, active filters, flexible ac transmission systems, and voltage compensators, which are only a few applications. For sinusoidal ac outputs, the magnitude, frequency, and phase should be controllable. According to the type of ac output waveform, these topologies can be considered as voltage source inverters (VSIs), where the independently controlled ac output is a voltage waveform. These structures are the most widely used because they naturally behave as voltage sources as required by many industrial applications, such as adjustable speed drives (ASDs), which are the most popular application of inverters.

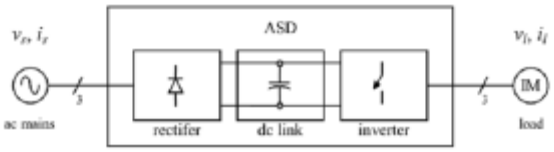

Fig 3.3.1 Basic Inverter Circuit

3.3.2 THREE PHASE INVERTER

Single-phase VSIs cover low-range power applications and three-phase VSIs cover the medium- to high-power applications. The main purpose of these topologies is to provide a three-phase voltage source, where the amplitude, phase, and frequency of the voltages should always be controllable. Although most of the applications require sinusoidal voltage waveforms (e.g., ASDs, UPSs, Var compensators), arbitrary voltages are also required in some emerging applications (e.g., active filters, voltage compensators).

The standard three-phase VSI topology is shown in Fig 3.3.2 and the eight valid switch states are given in Table 3.3.1.

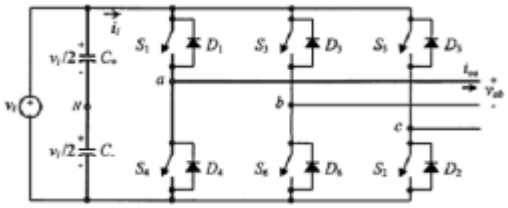

Fig 3.3.2 Three Phase VSI Topology

As in single-phase VSIs, the switches of any leg of the inverter (S1and S4, S3 and S6,or S5 and S2) cannot be switched on simultaneously because this would result in a short circuit across the dc link voltage supply. Similarly, in order to avoid undefined states in the VSI, and thus undefined ac output line voltages, the switches of any leg of the inverter cannot be switched off simultaneously as this will result in voltages that will depend upon the respective line current polarity. Of the eight valid states, two of them (7 and 8 in Table 3.3.1) produce zero ac line voltages. In this case, the ac line

www.ijetmas.com June 2015, Volume 3, Issue 6, ISSN 2349-4476

currents freewheel through either the upper or lower components. The remaining states (1 to 6 in Table 3.3.1) produce nonzero ac output voltages. In order to generate a given voltage wave-form, the inverter moves from one state to another. Thus the resulting ac output line voltages consist of discrete values of voltages that are vi, 0, and -vi. The selection of the states in order to generate the given waveform is done by the modulating technique that should ensure the use of only the valid states.

State	State #	v_{ab}	v_{bc}	v_{ca}
S_1, S_2, and S_6 are on and S_4, S_3, and S_5 are off	1	v_i	0	$-v_i$
S_2, S_3, and S_1 are on and S_5, S_6, and S_4 are off	2	0	v_i	$-v_i$
S_3, S_4, and S_2 are on and S_6, S_1, and S_5 are off	3	$-v_i$	v_i	0
S_4, S_5, and S_3 are on and S_1, S_2, and S_6 are off	4	$-v_i$	0	v_i
S_5, S_6, and S_4 are on and S_2, S_3, and S_1 are off	5	0	$-v_i$	v_i
S_6, S_1, and S_5 are on and S_3, S_4, and S_2 are off	6	v_i	$-v_i$	0
S_1, S_2, and S_3 are on and S_4, S_5, and S_6 are off	7	0	0	0
S_4, S_5, and S_2 are on and S_3, S_1, and S_6 are off	8	0	0	0

Table 3.3.1 Valid Switch states for a three phase VSI

For turning on the MOSFET in an inverter we need to provide a gate pulse for it. So in order to provide this gate pulse we are using a MOSFET Driver.

3.3.3 MOSFET DRIVER

To turn a power MOSFET on, the gate terminal must be set to a voltage at least 10 volts greater than the source terminal (about 4 volts for logic level MOSFETs). This is comfortably above the Vgsparameter.

One feature of power MOSFETs is that they have a large stray capacitance between the gate and the other terminals, Ciss. The effect of this is that when the pulse to the gate terminal arrives, it must first charge this capacitance up before the gate voltage can reach the 10 volts required. The gate terminal then effectively does take current. Therefore the circuit that drives the gate terminal should be capable of supplying a reasonable current so the stray capacitance can be charged up as quickly as possible. The best way to do this is to use a dedicated MOSFET driver chip.

Some require the MOSFET source terminal to be grounded (for the lower 2 MOSFETs in a full bridge or just a simple switching circuit). Some can drive a MOSFET with the source at a higher voltage. These have an on-chip charge pump, which means they can generate the 22 volts required to turn the upper MOSFET in a full bridge on.

Often you will see a low value resistor between the MOSFET driver and the MOSFET gate terminal. This is to dampen down any ringing oscillations caused by the lead inductance and gate capacitance which can otherwise exceed the maximum voltage allowed on the gate terminal. It also slows down the rate at which the MOSFET turns on and off. This can be useful if the intrinsic diodes in the MOSFET do not turn on fast enough.

3.4 MICROCONTROLER

Description:

The AT89C52 is a low-power, high-performance CMOS 8-bit microcomputer with 8Kbytes of Flash programmable and erasable read only memory (PEROM). The device is manufactured using Atmel's high-density nonvolatile memory technology and is compatible with the industry-standard 80C51 and 80C52 instruction set and pin out.

The on-chip Flash allows the program memory to be reprogrammed in-system or by a conventional nonvolatile memory programmer. By combining a versatile 8-bit CPUwith Flash on a monolithic chip, the Atmel AT89C52 is a powerful microcomputerwhich provides a highly-flexible and cost-effective solution to many embedded controlapplications.

Features

- Compatible with MCS-51 Products

www.ijetmas.com June 2015, Volume 3, Issue 6, ISSN 2349-4476

- 8K Bytes of In-System Reprogrammable Flash Memory
- Endurance: 1,000 Write/Erase Cycles
- Fully Static Operation: 0 Hz to 24 MHz
- Three-level Program Memory Lock
- 256 x 8-bit Internal RAM
- 32 Programmable I/O Lines
- Three 16-bit Timer/Counters
- Eight Interrupt Sources
- Programmable Serial Channel
- Low-power Idle and Power-down Modes

Fig 3.4.1 Microcontroller AT89C52

The AT89C52 provides the following standard features: 8K bytes of Flash, 256 bytes of RAM, 32 I/O lines, three 16-bit timer/counters, a six-vector two-level interrupt architecture, a full-duplex serial port, on-chip oscillator, and clock circuitry. In addition, the AT89C52 is designed with static logic for operation down to zero frequency and supports two software selectable power saving modes. The Idle Mode stops the CPU while allowing the RAM, timer/counters, serial port, and interrupt system to continue functioning. The Power-down mode saves the RAM contents but freezes the oscillator, disabling all other chip functions until the next hardware reset.

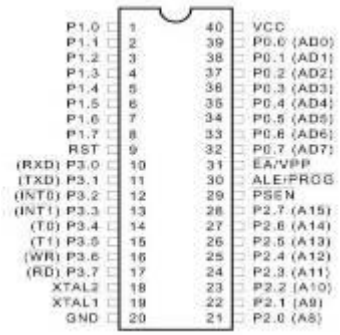

Fig 3.4.2 Pin Digram of AT89C52

4. CONTROL OF INVERTERS AND SVPWM TECHNIQUES

4.1 INTRODUCTION

The space vector PWM (SVM) method is an advanced, computation-intensive PWM method and is possibly the best among all the PWM techniques for variable-frequency drive applications. Because of its superior performance characteristics, it has been finding widespread application in recent years.

Considering implementation on a half bridge of a three phase bridge inverter, if the load neutral is connected to the center tap of dc supply all three half bridges operate independently, giving satisfactory PWM performance. With a machine load, the load neutral is normally isolated, which causes interaction among the phases. The SVM method considers this interaction of the phases and optimizes the harmonic content of the three-phase isolated neutral load. To understand the SVM theory, the concept of rotating space vector is important. If the three-phase sinusoidal and balanced voltages given by the equations

$$v_a = V_m \cos\omega t$$
$$v_b = V_m \cos\left(\omega t - \frac{2\pi}{3}\right) \qquad (4.1)$$
$$v_c = V_m \cos\left(\omega t + \frac{2\pi}{3}\right)$$

are applied to a three-phase induction, it can be easily shown that the space vector $\overline{V}$ with a magnitude V_m rotates in a circular orbit at angular velocity ω where the direction of rotation depends on the sequence of the voltages. With the sinusoidal three-phase command voltages, the composite PWM fabrication at the inverter output should be such that the average voltages with a minimum amount of harmonic distortion.

4.2PRINCIPLE OF SPACE VECTOR PWM

The circuit model of a typical three-phase voltage source PWM inverter is shown in

www.ijetmas.com June 2015, Volume 3, Issue 6, ISSN 2349-4476

Figure 4.1. S1 to S6 are the six power switches that shape the output, which are controlled by the switching variables a, a′, b, b′, c and c′. When an upper transistor is switched on, i.e., when a, bor c is 1, the corresponding lower transistor is switched off, i.e., the corresponding a′, b′ or c′ is 0. Therefore, the on and off states of the upper transistors S1, S3 and S5 can be used to determine the output voltage.

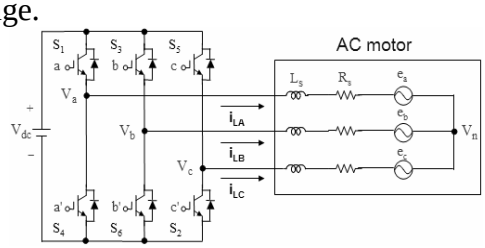

Figure 4.1 Three phase voltage source inverter

The relationship between the switching variable vector [a, b, c]^t and the line-to-line voltage vector [Vab Vbc Vca]^t is given by Equation 4.2

$$\begin{bmatrix} V_{ab} \\ V_{bc} \\ V_{ca} \end{bmatrix} = V_{dc} \begin{bmatrix} 1 & -1 & 0 \\ 0 & 1 & -1 \\ -1 & 0 & 1 \end{bmatrix} \begin{bmatrix} a \\ b \\ c \end{bmatrix} \qquad (4.2)$$

the relationship between the switching variable vector [a, b, c]t and the phase voltage vector [Va Vb Vc]^t can be expressed below.

$$\begin{bmatrix} V_{an} \\ V_{bn} \\ V_{cn} \end{bmatrix} = \frac{V_{dc}}{3} \begin{bmatrix} 2 & -1 & -1 \\ -1 & 2 & -1 \\ -1 & -1 & 2 \end{bmatrix} \begin{bmatrix} a \\ b \\ c \end{bmatrix} \qquad (4.3)$$

As illustrated in Figure. 4.1, there are eight possible combinations of on and off patterns for the three upper power switches. The on and off states of the lower power devices are opposite to the upper one and so are easily determined once the states of the upper power transistors are determined. According to equations (4.2) and (4.3), the eight switching vectors, output line to neutral voltage (phase voltage), and output line-to-line voltages in terms of DC-link V_{dc}, are given in Table 4.1 and Figure.4.2 shows the eight inverter voltage vectors (V0 to V7).

Voltage Vectors	Switching vector			Line to neutral voltage			Line to line voltage		
	a	B	C	Van	Vbn	Vcn	Vab	Vbc	Vca
V_0	0	0	0	0	0	0	0	0	0
V_1	1	0	0	2/3	-1/3	-1/3	1	0	1
V_2	1	1	0	1/3	1/3	-2/3	0	1	-1
V_3	0	1	0	-1/3	2/3	-1/3	-1	1	0
V_4	0	1	1	-2/3	1/3	1/3	-1	0	1
V_5	0	0	1	-1/3	-1/3	2/3	0	-1	1
V_6	1	0	1	1/3	-2/3	1/3	1	-1	0
V_7	1	1	1	0	0	0	0	0	0

(Note that respective voltage should be multiplied by Vdc)

Table 4.1 Switching vectors, phase voltages and output line to line voltages

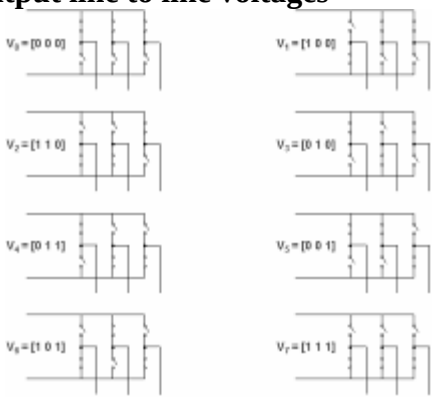

Fig 4.2 The eight inverter voltage vectors (V0 to V7)

4.3 IMPLEMENTATION OF SVM

Space Vector PWM (SVM) refers to a special switching sequence of the upper three power transistors of a three-phase power inverter. It has been shown to generate less harmonic distortion in the output voltages and or currents applied to the phases of an AC motor.ToimplementthespacevectorPWM,thevol

www.ijetmas.com June 2015, Volume 3, Issue 6, ISSN 2349-4476

tageequationsintheabcreferenceframe canbetransformedintothestationarydqreferencefr amethatconsistsofthehorizontal(d)and vertical(q)axes as depicted in Figure 4-3.

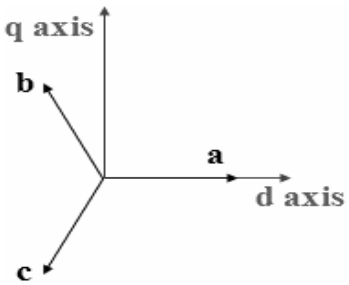

Fig 4.3 The relationship of abc reference frame and stationary dq reference frame

From this figure, the relation between these two reference frames is below

$\mathbf{f}_{dq0} = \mathbf{K}_S \mathbf{f}_{abc}$

where, $\mathbf{K}_S = \frac{2}{3}\begin{bmatrix} 1 & -1/2 & -1/2 \\ 0 & \sqrt{3}/2 & -\sqrt{3}/2 \\ 1/2 & 1/2 & 1/2 \end{bmatrix}$, $\mathbf{f}_{dq0}=[f_a$ f_b $f_c]^T$, and f denotes either a voltage or a current variable.

As described in Figure.4-3, this transformation is equivalent to an orthogonal projection of $[a\ b\ c]^t$ on to the two-dimensional perpendicular to the vector$[1,1,1]^t$(the equivalent d-q plane)in a three-dimensional coordinate system. As a result, six non-zero vectors and two zero vectors are possible. Six nonzero vectors (V1 - V6)shape the axe so hexagonal as depicted in Figure 4-4,and feed electric power to the load. The angle between an y adjacent two non-zerovectorsis60 degrees Mean while, two zero vectors(V0 and V7)are at the origin and apply zero voltage to the load. The eight vectors are called the basics pace vectors and are denoted by V0, V1, V2, V3, V4, V5, V6, and V7. The same transformation can be applied to the desired output voltage to get the desired reference voltage vector Vref in the d-q plane.

The objective of space vector PWM technique is to approximate the reference voltage vector Vref using the eight switching patterns. One simple method of approximation is to generate the average output of the inverter in a small period T, to be the same as that of Vref in the same period.

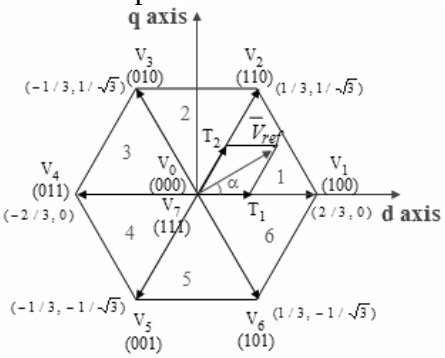

Fig 4.4 Basic switching vectors and sectors.

Therefore, space vector PWM can be implemented by the following steps:

Step 1. Determine Vd, Vq, Vref, and angle α

Step 2. Determine time duration T1, T2, T0

Step 3. Determine the switching time of each transistor (S1 to S6)

Step1: Determine Vd, Vq, Vref and α

From Figure. 4-5, the Vd, Vq, Vref, and angle can be determined as follows:

$$\begin{bmatrix} V_d \\ V_q \end{bmatrix} = \frac{2}{3}\begin{bmatrix} 1 & -1/2 & -1/2 \\ 0 & \sqrt{3}/2 & -\sqrt{3}/2 \\ 1/2 & 1/2 & 1/2 \end{bmatrix}\begin{bmatrix} V_{an} \\ V_{bn} \\ V_{cn} \end{bmatrix} \quad (4.4)$$

$$|V_{ref}| = \sqrt{V_d^2 + V_q^2} \quad (4.5)$$

$$\alpha = \tan^{-1}\left(\frac{V_q}{V_d}\right)$$

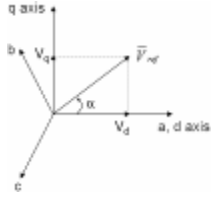

Fig 4.5 Voltage Space Vector and its components in (d, q)

www.ijetmas.com June 2015, Volume 3, Issue 6, ISSN 2349-4476

Switching time duration at Sector 1

$$\int_0^{T_z} \overline{V}_{ref} = \int_0^{T1} \overline{V}_1 dt + \int_{T1}^{T1+T2} \overline{V}_2 dt + \int_{T1+T2}^{T_z} \overline{V}_0 dt$$

(4.6)

$$T_z.\overline{V}_{ref} = (T_1.\overline{V}_1 + T_2.\overline{V}_2)$$

$$T_z.|\overline{V}_{ref}|.\begin{bmatrix}\cos\alpha \\ \sin\alpha\end{bmatrix} = T_1.\frac{2}{3}.V_{dc}\begin{bmatrix}1 \\ 0\end{bmatrix} + T_2.\frac{2}{3}.V_{dc}.\begin{bmatrix}\cos(\Pi/3) \\ \sin(\Pi/3)\end{bmatrix}$$

(Where $0 \le \alpha \le 60^0$)

$$T_1 = \frac{\sqrt{3}*T_Z*|V_{ref}|}{V_{dc}}\left(\sin\left(\frac{\pi}{3}-\alpha\right)\right)$$

$$T_2 = \frac{\sqrt{3}*T_Z*|V_{ref}|}{V_{dc}}(\sin\alpha)$$

$$T_0 = T_z - T_1 - T_2;$$

Similarly for n'th sector

$$T_1 = \frac{\sqrt{3}*T_Z*|V_{ref}|}{V_{dc}}\left(\sin\left(\frac{\pi}{3}-\alpha+\frac{n-1}{3}\pi\right)\right)$$

$$= \frac{\sqrt{3}*T_Z*|V_{ref}|}{V_{dc}}\left(\sin\frac{n}{3}\pi-\alpha\right) \quad (4.7)$$

$$= \frac{\sqrt{3}*T_Z*|V_{ref}|}{V_{dc}}\left(\sin\frac{n}{3}\pi*\cos\alpha-\cos\frac{n}{3}\pi*\sin\alpha\right)$$

$$T_2 = \frac{\sqrt{3}*T_Z*|V_{ref}|}{V_{dc}}\left(\sin\left(\alpha-\frac{n-1}{3}\pi\right)\right)$$

$$= \frac{\sqrt{3}*T_Z*|V_{ref}|}{V_{dc}}\left(-\sin\frac{n-1}{3}\pi*\cos\alpha+\cos\frac{n-1}{3}\pi*\sin\alpha\right)$$

(4.8)

$$T_0 = T_z - T_1 - T_2$$

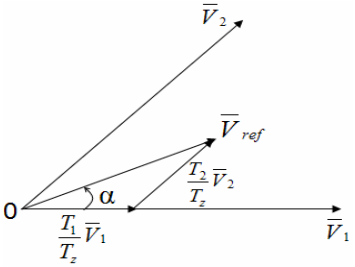

Fig 4.6 Reference vector as a combination of adjacent vectors at sector 1

Step 2: Determine the switching time of each transistor (s1 to s6) shows space vector PWM switching patterns at each sector.

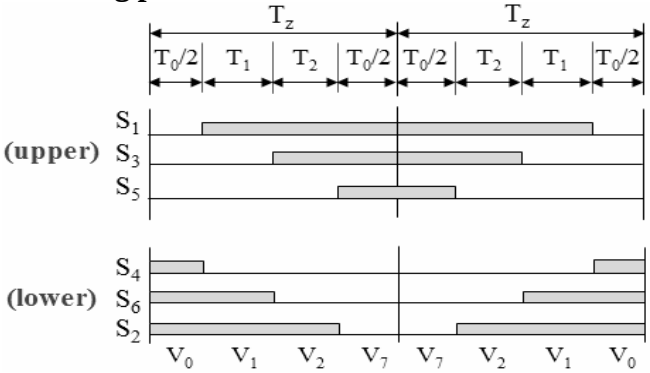

Fig 4.7 switching patterns at Sector 1

Based on Figure.4-7,the switching time at each sector is summarized in Table2, and it will be built in SIMULINK model to implement SVPWM.

Sector	Upper Switches (S_1, S_3, S_5)	Lower Switches (S_4, S_6, S_2)
1	$S_1 = T_1 + T_2 + T_0/2$ $S_3 = T_2 + T_0/2$ $S_5 = T_0/2$	$S_4 = T_0/2$ $S_6 = T_1 + T_0/2$ $S_2 = T_1+T_2+T_0/2$
2	$S_1 = T_1 + T_0/2$ $S_3 = T_1 + T_2 + T_0/2$ $S_5 = T_0/2$	$S_4 = T_2 + T_0/2$ $S_6 = T_0/2$ $S_2 = T_1+T_2+T_0/2$
3	$S_1 = T_0/2$ $S_3 = T_1 + T_2 + T_0/2$ $S_5 = T_2 + T_0/2$	$S_4 = T_1+T_2+T_0/2$ $S_6 = T_0/2$ $S_2 = T_1 + T_0/2$
4	$S_1 = T_0/2$ $S_3 = T_1 + T_0/2$ $S_5 = T_1 + T_2 + T_0/2$	$S_4 = T_1+T_2+T_0/2$ $S_6 = T_2 + T_0/2$ $S_2 = T_0/2$
5	$S_1 = T_2 + T_0/2$ $S_3 = T_0/2$ $S_5 = T_1 + T_2 + T_0/2$	$S_4 = T_1 + T_0/2$ $S_6 = T_1+T_2+T_0/2$ $S_2 = T_0/2$
6	$S_1 = T_1 + T_2 + T_0/2$ $S_3 = T_0/2$ $S_5 = T_1 + T_0/2$	$S_4 = T_0/2$ $S_6 = T_1+T_2+T_0/2$ $S_2 = T_2 + T_0/2$

Table 4.2 Switching Time Calculation at Each Sector

5. SIMULATION BLOCK DIAGRAMS AND RESULTS

5.1. MATLAB SIMULATION CIRCUIT:

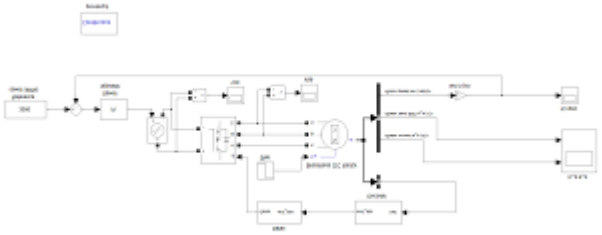

www.ijetmas.com June 2015, Volume 3, Issue 6, ISSN 2349-4476

Fig 5.1 MATLAB Simulation Diagram

5.2 HALL SENSORS SUB CIRCUIT:

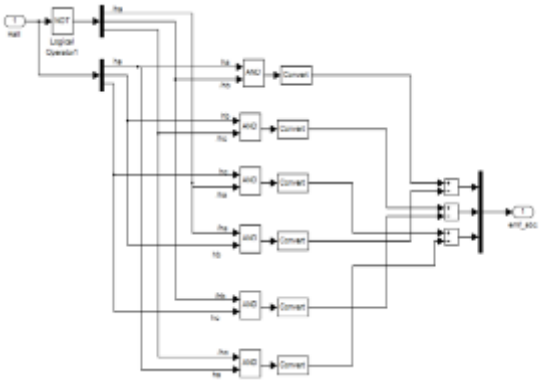

Fig 5.2 Hall Sensors SubCircuit

5.2.1 Truth Table Implementation for Hall Sensor Sub-Circuit:

Ha	Hb	Hc	Emf_a	Emf_b	Emf_c
0	0	0	0	0	0
0	0	1	0	-1	1
0	1	0	-1	1	0
0	1	1	-1	0	1
1	0	0	1	0	-1
1	0	1	1	-1	0
1	1	0	0	1	-1
1	1	1	0	0	0

Table 5.1

5.3 Gate Signals Sub Circuit:

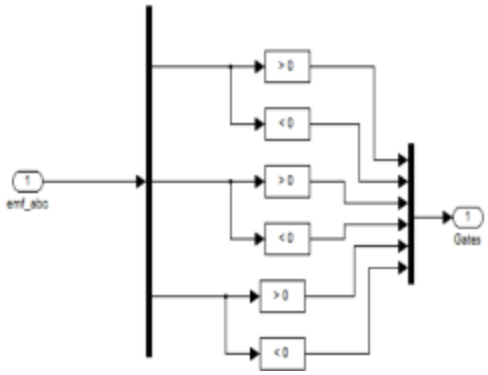

Fig 5.3 Gate signals sub circuit

5.3.1 Truth Table for generating the Gate pulses:

Emf_a	Emf_b	Emf_c	Q1	Q2	Q3	Q4	Q5	Q6
0	0	0	0	0	0	0	0	0
0	-1	1	0	0	0	1	1	0
-1	1	0	0	1	1	0	0	0
-1	0	1	0	1	0	0	1	0
1	0	-1	1	0	0	0	0	1
1	-1	0	1	0	0	1	0	0
0	1	-1	0	0	1	0	0	1
0	0	0	0	0	0	0	0	0

Table 5.2

5.4 Output Waveforms:

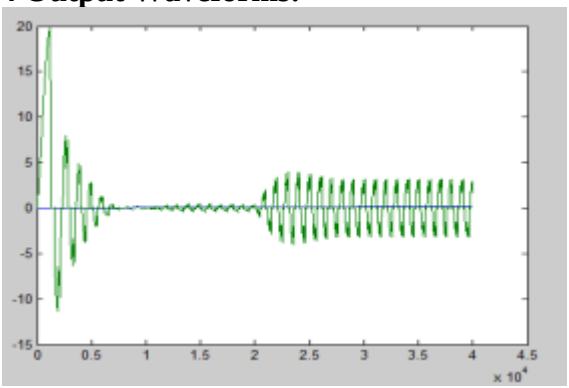

x-axis :- Time (sec) y-axis :- stator current (ampere)

Fig 5.4 Stator currents

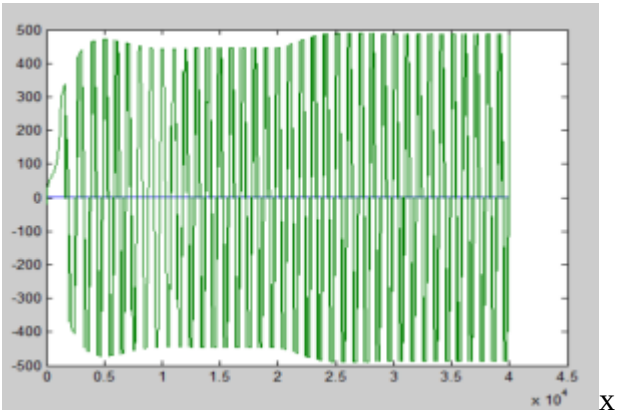

x-axis :- Time (sec) y-axis :- stator EMF(volt)

Fig 5.5 bldc stator emf

www.ijetmas.com June 2015, Volume 3, Issue 6, ISSN 2349-4476

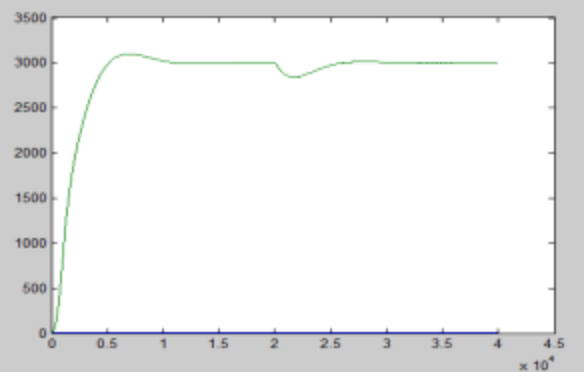

x-axis :- Time (sec) y-axis :- Speed (RPM)

Fig 5.6 Speed Characteristics of bldc

6. HARDWARE IMPLEMENTATION

The aim of the project is to control the speed of a BLDC motor using a microcontroller with the help of SVPWM-technique. As far as the hardware implementation is concerned, it is implemented for open loop of operation.

6.1BLOCK DIAGRAM

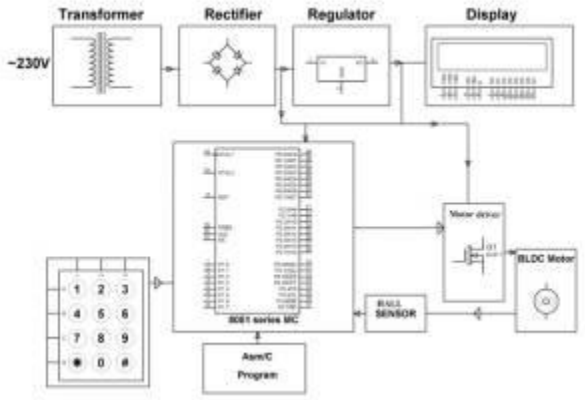

Fig 6.1 Block diagram

The entire power required is drawn from a single phase AC Source. This source is used to derive gate driving voltages for the motor driver, control circuit operating voltage and finally to drive the motor through motor driver bridge.

6.2 CIRCUIT SPECIFICATIONS

This section covers a BLDC motor drive controlled by microcontroller with the following specifications.

- Input : 12 volts to Motor Driver
- BLDC Motor AT2212 Motor
- Microcontroller: AT89C52
- Hall Sensors : 17X131
- Motor Driver : HW30A

6.3 OPERATION

The operation of the circuit can be explained in three parts.

1. Control circuit:

This gives out the switching signals to the converter bridge. A microcontroller is dedicated to generate the switching pulses. The microcontroller is programmed to give out pulse according to SVPWMM technique.

Program is compiled in Keil software. The HEX code generated is loaded into the Microcontroller. The controller used is AT89C52. The controller is operated at 11.059 MHz frequency.

2. Motor driver and Gate driving circuit:

Instead of using an inverter and a regulator we have used a motor driver HW30A which acts as inverter to supply the voltage for the Motor. HW30A is an inbuilt Inverter which is having Inverter circuit as well as MOSFET Driver circuit. We are using this type of technique because of on using general inverter we are facing the difficulties like large Heat dissipation, so that this heat would cause a heat sinking problem which in turn results in the failure of the Inverter. SO, by using this motor driver the circuit complexity is reduced and the heat dissipation problem, is also reduced.

3. Converter circuit:

The converter circuit is provided by the Motor driver. The D.C supply is fed through a bridge rectifier. The switches in the Motor driver are turned ON and OFF as per the program. The Motor Drive is capable carrying a continuous current of 30A at 25 degree centigrade.

The rectifier circuit is made of diodes. The component used is IN4007 which is

www.ijetmas.com June 2015, Volume 3, Issue 6, ISSN 2349-4476

capable of blocking a reverse voltage of 1000 V DC and can carry a current of 10A continuous. All these components are placed on General PCB.Control circuit and gate driving circuit components are soldered directly on the pcb, whereas, the power components as connected with suitable connectors as they carry larger currents.

6.3 OPERATION

Hall Sensors senses the magnetic field means when North pole of a magnet is nearer to the sensor it gives output is high and when south pole of a magnet is nearer to the sensor it gives output is low we connect resistor between input and output terminal as shown in figure and output is shown with the help of LED and output value is measured with the help of multimeter.

In BLDC motor , supply given to the stator depend upon the rotor position and rotor position is sensed by the hall sensor and the output of the hall sensor output is given as input to the microcontroller. We use three hall sensors and the outputs of the three hall sensors are given as input to microcontroller

With the help of microcontroller we generate six waveforms for the three phase inverter circuit in120 degrees of mode of operation (output is six stepped waveform). Depends upon the rotor position microcontroller gives two pulses only means when one pulse is going to be OFF, at the same time another pulse is ON.

The output pulses from the microcontroller is 5V and it is not sufficient to drive the MOSFET gate so we need to place the driver circuit for increasing the magnitude and to maintain the constant value in higher magnitude because gate pulse is maintained constant for the full time. When gate pulse is removed Mosfet turns off. Instead of using inverter and MOSFET driver we are using a Motor Driver HW30A.

7. CONCLUSIONS

By this paper, the working of BLDC motor which is controlled by microcontroller is shown. Simulation of the inverter is done on the MATLAB Simulink. BLDC motors possess high efficiency. In BLDC motor PM are on the rotor & electromagnets are on the stator controlled by software.

8. REFERENCES

- Development of Microcontroller Based SpeedControl Scheme of BLDC Motor Using Proteus VSM Software International Journal of Electronics and Electrical Engineering Vol. 2, No. 1, March, 2014
- A. Emadi, A. Sathyan, N. Milivojevic, Y-J. Lee, and M.Krishnamurthy, “An FPGA-Based novel digital pwm control scheme for BLDC motor drives,” IEEE Transactions on IndustrialElectronics, vol. 56, no. 8, August 2009.
- P.Pillay ad R.Krishnan, “Modeling, Simulation and Analysis of a Permanent Magnet Brushless DC motor drive part II: The brushless DC motor drive,” IEEE Transactions on Industry application, Vol.25, May/Apr 1989.
- V.H.Prasad D. Boroyevich and R. Zhang,“Analysis and Comparison of Space Vector ModulationSchemes for Three-Leg and Four Leg Voltage Source Inverters,” IEEE AppliedPower Electronics Conference and Exposition, Vol. 2, pp. 864-871, February1997.
- F. Rodriguez and A. Emadi, “A novel digital control technique forbrushless DC motor drives: Steady state and dynamics,” in Proc.IEEE Ind. Electron. Conf., Nov 2006, pp. 1545–1550.
- A.W. Leedy, and R.M. Nelms, “Harmonic Analysis of a Space Vector PWM Inverter using the Method of Multiple Pulses,” IEEE Transactions on

www.ijetmas.com June 2015, Volume 3, Issue 6, ISSN 2349-4476

Industrial Electronics,Vol. 4, pp. 1182-1187, July 2006.

- S.X. Chen, M.A. Jabbar, O.D. Zhang and Z.J. Lie. 1996. New Challenge: Electromagnetic design of BLDC motors for high speed fluid film bearing spindles used in hard disk drives. IEEE Trans. Magnetics. l32(5): 3854-3856, Sep.
- M. George and A. R. Paul, "Brushless DC motor control using digital PWM techniques," in Proc. International Conference on Signal Processing, Communication, Computing and Networking Technologies, 2011.
- J.D. Ede, Z.Q. Zhu and D. Howe. 2001. Optimal split ratio control for high speed permanent magnet brushless DC motors. In: Proceeding of 5thInternetaional Conference on Electrical Machines and Sytems. 2: 909-912.
- M. Nasrul, A. Satar, and D. Ishak, "Application of proteus VSM in modelling brushless DC motor drives," in Proc. 4th International Conference on Mechatronics, IEEE, Kuala Lumpur, Malaysia, May17-19, 2011.
- B.K. Bose. Modern Power Electrics and AC Drives. Prentice-Hall, Inc., 2002.